

Report of the DESY Summer Student Program 2006:

**Simulation of the Compton Polarimeter
for the International Linear Collider**

by

Daniel Asmus

University of Kiel

15.09.2006

Contents

1	Introduction	3
2	General Design and Layout	3
3	Theoretical and Technical Aspects	4
3.1	Compton Polarimetry	4
3.1.1	Statistical Errors	6
3.2	Cerenkov Radiation	7
3.3	Photomultipliers	9
3.3.1	Operating Parameters	9
4	The Program	10
4.1	Structure	10
4.2	Short Description of the classes	10
4.3	Operation	11
5	Results	13
5.1	Systematical Errors	16
6	Summary	16
7	Appendix: The Steering File	17
8	References	18

1 Introduction

The high energy physics (HEP) experiments at the future International Large Collider (ILC) will need a high beam polarization because the cross sections for the physical processes observed depends on the longitudinal spin directions of the beams at the interaction point (IP). Additionally some properties of the elementary particles can only be observed at high polarization. Therefore the measurement of the polarization with high precision ($\frac{\Delta P}{P} = 0.25\%$) is very important. For the ILC a polarization of 80% for the electrons beam is scheduled (and 60% for the positron beam optionally). The proposed device for the measurement is a Compton polarimeter (CP) which in general has the similar design of the detector as the one of the old TESLA project. The aim of this Monte Carlo simulation is to test different designs in detail and examine the systematical errors which can be expected.

2 General Design and Layout

At the ILC the polarized electrons are produced by shooting circularly polarized laser light into a GaAs cathode and after that they are split into smaller bunches before passing the pre-accelerator linac. The process used for the polarized positrons is much more complicated. The polarimeter will presumably be placed round about 600 meters upstream of the IP. At this point the beam and spin directions of the electrons are aligned with those at the detector location. The concept of the polarimeter is based on Compton scattering of the electrons with

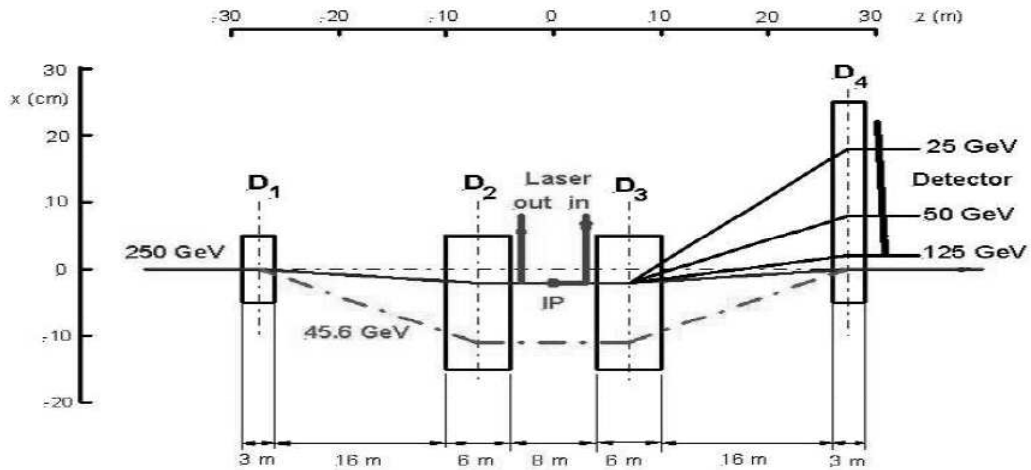


Figure 1: Layout of Polarimeter as a 4-magnet chicane ([2])

the use of a pulsed laser beam whereas the helicity of the laser can be selected pulse wise. Just after the laser crossing there is a dipole magnet which bends the scattered electrons. So the electrons with different energies are separated in space before they reach the detector array which consists of Cerenkov gas tubes in front of photomultipliers. The longitudinal polarization then is determined from the asymmetry of two measurements with parallel and anti-parallel spin configurations of the interacting electron and laser beams. This detection method and the parameters in detail have to be investigated.

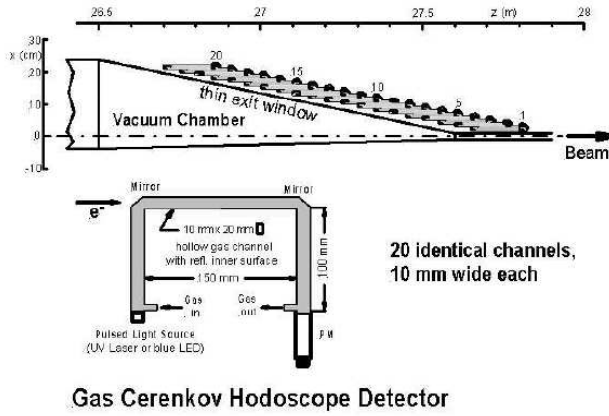


Figure 2: Cerenkov detector layout ([2]).

3 Theoretical and Technical Aspects

3.1 Compton Polarimetry

In this section the basic features of the Compton scattering process and polarization are mentioned. First one introduces the the dimensionless variable

$$x = \frac{4E_0\omega_0}{m_e^2} \cos^2(\theta_0/2) \simeq \frac{4E_0\omega_0}{m_e^2} \quad (1)$$

where E_0 the initial electron energy, ω_0 the initial photon energy and θ_0 the crossing angle between the electron beam and the laser. This is rather small so that $\cos(\theta_0/2) \simeq 1$ for most practical polarimeter cases. Because of energy conservation the following relation between the energies before and after the scattering must be true

$$\omega + E = \omega_0 + E_0 \simeq E_0 \quad (2)$$

where E_0 is much more bigger and therefore dominates. Nevertheless the energy spectra are continuous and directly related. So that at the Compton edge the maximum energy of the scattered photon corresponds to the minimum of the energy of the electron

$$\omega_{max} = E_0 \frac{x}{1+x} \quad (3)$$

$$E_{min} = E_0 \frac{1}{1+x} \quad (4)$$

The scattered photon and electron angles relative to the original beam direction are

$$\theta_\gamma = \frac{m_e}{E_0} \sqrt{\frac{x}{y} - (x+1)} \quad (5)$$

$$\theta_e = \frac{y}{1-y} \theta_\gamma \quad (6)$$

where

$$y = 1 - \frac{E}{E_0} = \frac{\omega}{E_0} \quad (7)$$

is the normalized energy variable of the scattered photon. Then the spin dependent differential Compton cross section is given by

$$\frac{d\sigma}{dy} = \frac{2\sigma_0}{x} \left[\frac{1}{1-y} + 1 - y - 4r(1-r) + P\lambda rx(1-2r)(2-y) \right] \quad (8)$$

where P is the initial electron helicity with $(-1 \leq P \leq +1)$, λ is the initial photon helicity with $(-1 \leq \lambda \leq +1)$, and

$$\sigma_0 = \pi r_0^2 = 0.2495 \text{ barn} \quad (9)$$

$$r = \frac{y}{x(1-y)} \quad (10)$$

With these parameters one can define the spin asymmetry

$$A = \frac{d\sigma^- - d\sigma^+}{d\sigma^- + d\sigma^+} \quad (11)$$

where the (-) and the (+) correspond each to the product of the beam helicities $P\lambda = \pm 1$. The configuration with $P\lambda = -1$ dominates at the Compton edge, therefore the asymmetry is positive in this region. But it changes sign at the crossover points

$$\omega_{cross} = E_0 \frac{x}{2+x} \quad (12)$$

$$E_{cross} = E_0 \frac{1}{1+x/2} \quad (13)$$

which coincide with the point where the maximum electron scattering angle is attained. The longitudinal beam polarization P of the electron beam could be determined from the asymmetry A and the analyzing power A_p assuming a perfect laser helicity

$$P = \frac{A}{A_p} \quad (14)$$

where the analyzing power is $A_p = A(P = 1)$. The kinematics of the scattering process is completely determined by obtaining the parameters of only one of the final state particles.

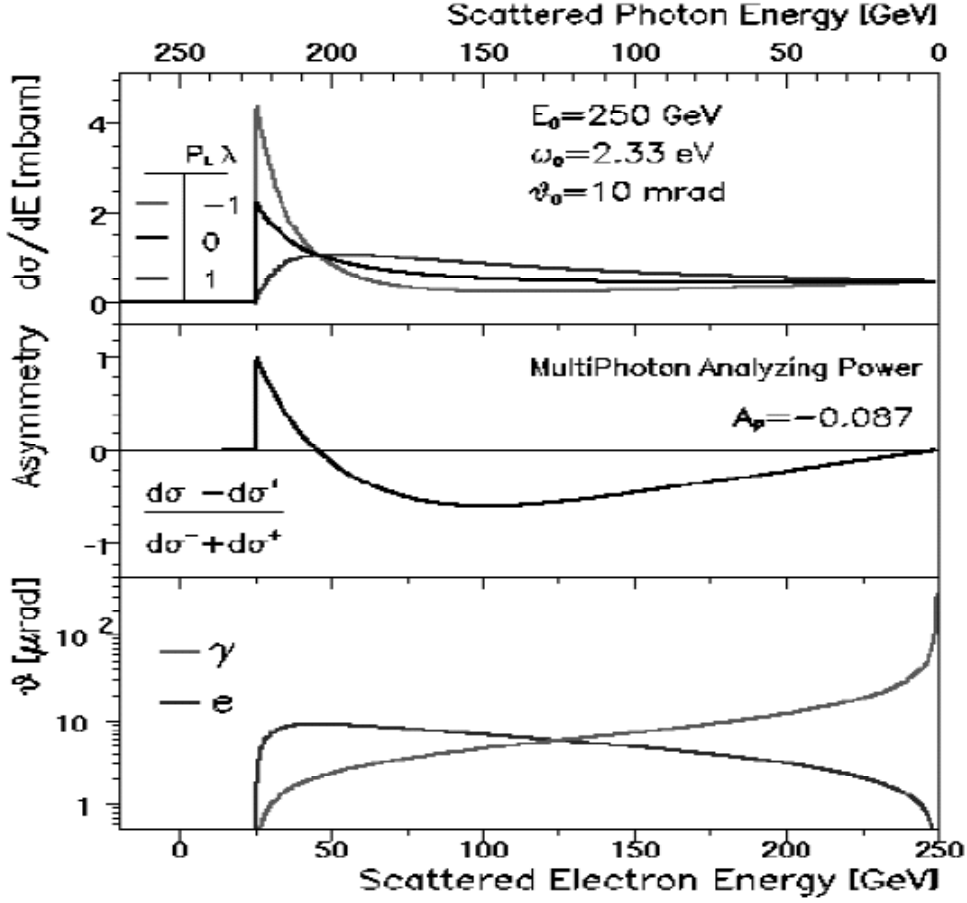


Figure 3: Energy spectra (top), spin asymmetry (middle) and scattering angle (bottom) of Compton scattered electrons and photons.([1])

3.1.1 Statistical Errors

There were already been done studies of the statistical errors so that is not in the focus of this work. Therefore only a short view on this topic.

The longitudinal beam polarization is determined from the experimental measurements N_1 and N_2 which give the event statistics with the two different helicity configurations

$$P = \frac{1}{A_p} \frac{N_1 - N_2}{N_1 + N_2} \quad (15)$$

With this relation the statistical error of the measured beam polarization can be derived through error propagation

$$\frac{\Delta P}{P} = \frac{1}{\sqrt{\sum_i w_i (N_{1i} + N_{2i})}} = \frac{1}{\sqrt{\Delta t \sum_i w_i R_i}} \quad (16)$$

where the sum is over all bins i , $R_i = (N_{1i} + N_{2i})/\Delta t$ is the event rate in energy bin i , Δt is the measurement time required for a certain statistical precision and

$$w_i = \frac{1}{1 + P^{-2} A_i^{-2}} \quad (17)$$

are the statistical weights. There has been already calculations done ($\Delta P/P = 0.082\%$ for $dT = 1 \text{ sec}$) which show that the genuine statistical errors from the event statistics will be exceedingly small and negligible in comparison with systematic effects.

3.2 Cerenkov Radiation

This section gives a brief review on the radiation emitted by a charged particle moving through a medium faster than the speed of light in this medium. This velocity threshold is given by

$$\beta c \geq c/n \quad (18)$$

where n is the refraction index and c the speed of light in vacuum. In case the particle travels

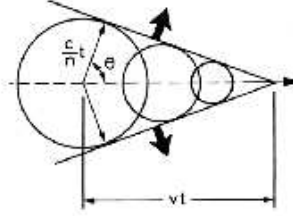


Figure 4: Cerenkov Radiation

faster than an electromagnetic wave. It is created just like a sonic shock wave in air. The conical wavefront is emitted in a well-defined angle to the direction of the particle momentum

$$\cos\theta_{Cer} = \frac{1}{\beta n(\omega)} \quad (19)$$

From this with a longer calculation the number of photons emitted per unit wavelength per unit length of the radiator is

$$\frac{d^2 N}{d\lambda dx} = \frac{2\pi z^2 \alpha}{\lambda^2} \left(1 - \frac{1}{\beta n(\lambda)} \right) \quad (20)$$

where Z is the number of elementary charges, α , the fine structure constant and ω the frequency.

The over the path length integrated function of (20) is shown in Figure 5. For the proposed detector the total number of photons emitted is also interesting. Integration over all sensible wavelengths and the length of the radiator gives this total number assuming a constant refraction index

$$N = 2\pi L \alpha \left(1 - \frac{1}{n^2} \right) \left[-\frac{1}{\lambda} \right]_{\lambda_{min}}^{\lambda_{max}} \quad (21)$$

where λ_{min} and λ_{max} give the interesting wavelength interval.

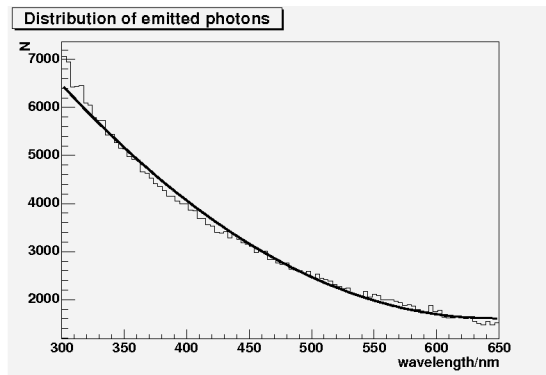


Figure 5: Cerenkov Radiation: $\frac{dN}{d\lambda}$ analytical and calculated with Monte Carlo.

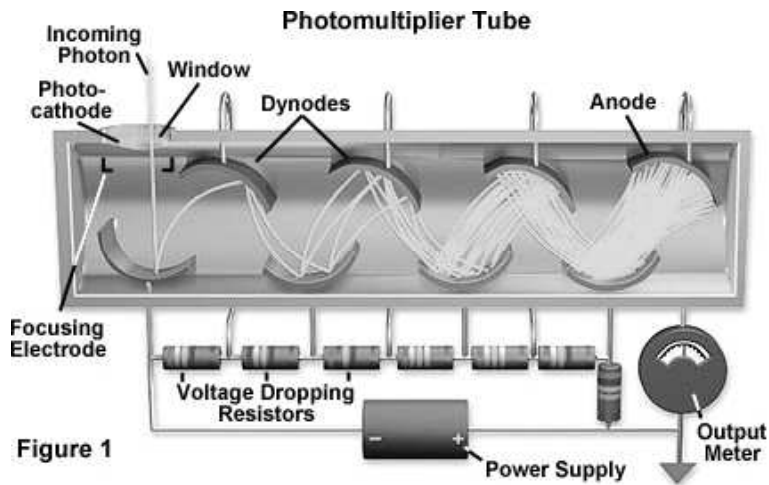


Figure 6: working principle of a PM

3.3 Photomultipliers

For the detection of the electron most likely a photomultiplier (PM) tube will be used as in the actual proposal. There are some characteristics all photomultipliers have in common. A typical device consists of a cathode made of photosensitive material followed by an electron collection and multiplier system (the dynodes) and an anode where the final signal is taken. During operation a high voltage is applied to all the parts in a potential "ladder". When an incoming photon hits the photo-cathode an electron is emitted (photoelectric effect). The efficiency for the photoelectric conversion varies strongly with the wavelength of the incident photon. This overall spectral response is expressed by the quantum efficiency ($\eta(\lambda)$). The emitted electron is accelerated by the supply voltage toward the first dynode and when it hits the dynode secondary electrons are emitted. This causes an avalanche of electrons getting bigger at every dynode finally hitting the anode. In the optimal case the current measured at the anode is directly proportional to the number of incident photons. However in reality there are many effects which cause deviation from linearity.

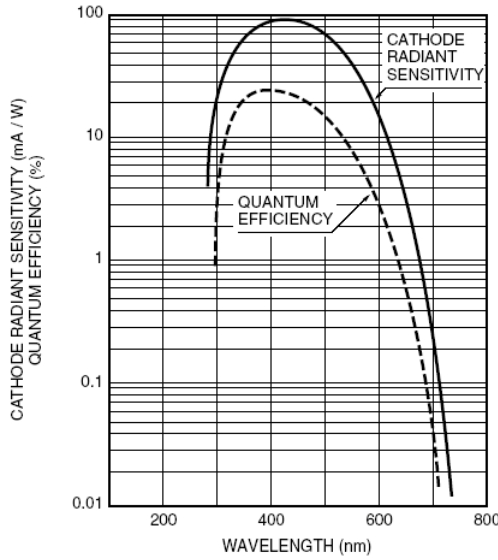


Figure 7: Spectral Response of R6094

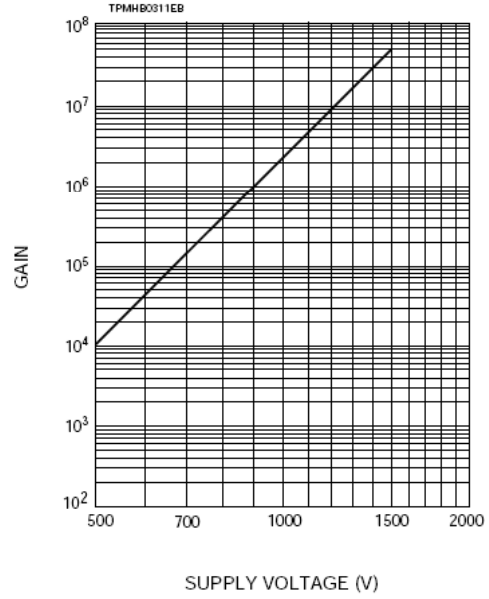


Figure 8: Gain of R6094

3.3.1 Operating Parameters

the overall amplification factor or gain (G) of a PM depends on the number of dynodes (n) and the applied supply voltage (V)

$$G = K \cdot V^{n\alpha} \quad (22)$$

where K is a proportionality constant depending on the material of the dynodes and the voltage division between them and $0.6 \leq \alpha \leq 0.8$. Here it is assumed that all dynodes have the same secondary emission factor (δ). Variation of the supply voltage have strong effects on the gain as can be seen in the following relation

$$\frac{dG}{G} = n\alpha \frac{dV}{V} \quad (23)$$

The important properties quantum efficiency and gain as functions of wavelength and supply voltage are shown in *Figure 7* and *Figure 8* for the uses PM tube Hamamatsu R6094/6095. There are many other properties of the PM which are not implemented in the program jet.

4 The Program

4.1 Structure

The program has to include many components like the electron and laser beams, the spectrometer and the detector. The Compton Scattering must be calculated. After that the simulation of the path and detection of the electrons is necessary. And finally the last step is the creation of the Cerenkov photons in the gas channels and their detection at the PM.

The simulation has to work on different levels: For each electron which scatters the energy and path through the magnetic spectrometer has to be calculated. Then the electrons reach the detector array and most of them are detected and sorted in the different channels. After that the Cerenkov radiation in the Gas tubes have to be detected for each of the bunch crossings. The measurement of the beam polarization actually happens after a certain time during which many crossings occur. however the goal of the simulation is to test different detector designs and therefore there must be the possibility to change single components of the polarimeter/program. These demands define the overall structure of the program. It is object oriented so that every detector component is implemented in its own class. There are limitations to this ideal structure because of some properties of for example the photomultiplier which are also needed in the gas tube to calculate the number of photons created in the detectable range of the PM. Therefore the gas tube and the PM share the same class.

However the type of the output of the simulation can be selected: An output readable by ROOT or Paw is possible. The structures (tree or hbook) are created at the beginning of the program.

4.2 Short Description of the classes

Before the Simulation can begin the starting parameters like beam energies and dimensions of the spectrometer or the used PM have to be set. This happens via a steering file which contains all this information. To read out the steering file and to create the keywords of the parameters the class *Cread* is used.

all the other classes are necessary for the real simulation. For the laser beam there is the class *Laser* which holds all important functions and parameters as energy, number of particles per pulse and crossing angle of the pulsed laser beam.

The class *EBeam* does the same for the electron beam. To calculate the Compton Scattering the program uses the *ComptonGenerator* class. It has the two beams as input and its functions give back the parameters of the electrons after the scattering. Next class is the *Spectrometer* which implements the magnetic spectrometer containing the last two dipole magnets of the chicane. Here the path through these magnets and the coordinates of the scattered electrons at the end of the last magnet are determined. The last class up to now is the *Detector* mother class holding all basic functionalities and properties of the detector used to detect the scattered electrons. It has already one child class the *GasDetector* which presents the up-to-date Gas Cerenkov detector array consisting of the gas tube and the PM. Here the creation of Cerenkov photons and the application of the quantum efficiency happens. Its main function is *detect* executing these physical processes and filling the member arrays which hold the numbers of the Cerenkov photons and photo electrons.

At first there were attempts to implement the photomultipliers in its own class called *Photodetector* but because of the given reasons this failed and is not in use right now.

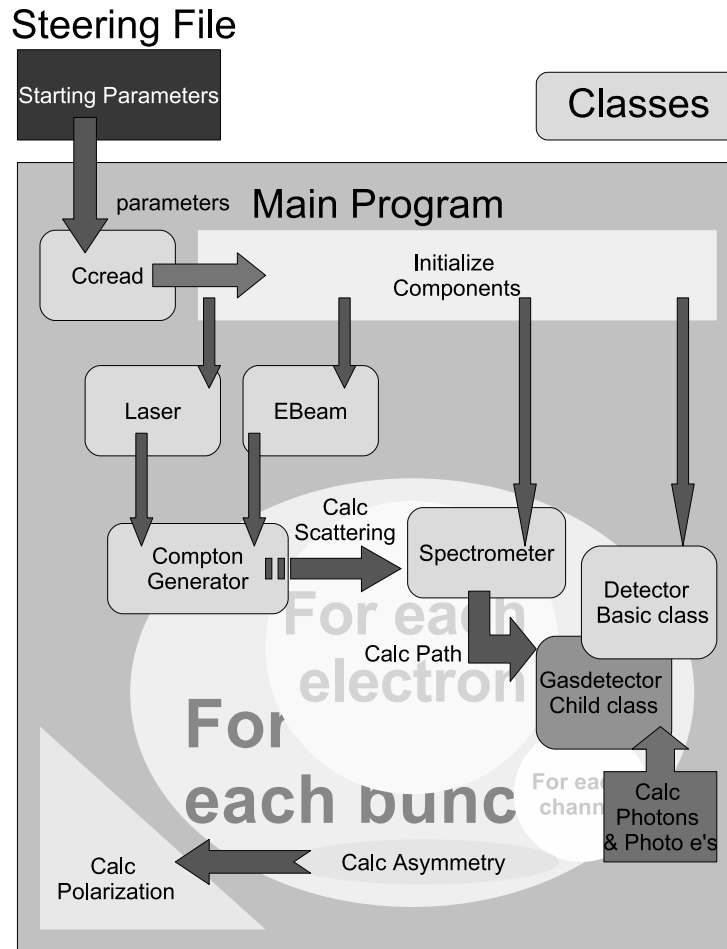


Figure 9: Structure of the program

4.3 Operation

As already mentioned above the starting parameters of the program are set up in an extra steering file so they can easily be changed by the user. At the beginning of the program the parameters are read out and the different objects for the electron, the laser beam and the spectrometer and the detector are initialized. After that the analyzing power of the detector configuration is determined. now the following steps are done for each simulated bunch crossing:

The mean of the Compton interaction and its Poisson distribution is calculated for the scattering with the Compton generator class. Next the path of each electron through the spectrometer is simulated and its coordinates at the end are calculated. This is all being done by the spec-

trometer class. After that the electrons are sorted into the detector channels or go undetected. In the next steps the program switches to another level where the emittance of the Cerenkov photons and the application of the quantum efficiency of the PM happens only for each crossing and channel. At the end of the program the output is written in a ROOT tree in an extra file and the asymmetry, errors and polarization can be calculated. It is planned to implement the remaining properties of the PM and the electronics to complete the simulation but this is still in progress.

5 Results

There have been done some first simulations with the applied quantum efficiency of the PM. For that the data of the Hamamatsu R6094 PM and the up to date chicane design with the TESLA detector have been used.

Important Input Parameters

electron energy	250 GeV
laser energy	2.33 eV
electron polarization	0.8
electrons per bunch	10^{10}
bunches per train	2820
dipole magnetic field	0.4804 T
refraction index of gas	1.0014
wavelength range of PM	300 - 650 nm
measuring time	1 s

In the following histograms one can see the spacial and energy distributions of the electrons for the different helicity configurations at different stages during their path through the Compton polarimeter. Just after the scattering all electrons are spread in a small region (*Figure 10*). The energy asymmetry of the scattering process which can be seen in *Figure 11* and *Figure 12* is transformed into a spacial asymmetry by the magnetic spectrometer (*Figure 13 & 14*). When the electrons finally reach the detector they are divided in the channels as the last two histograms show for the two configurations (*Figure 15 & 16*).

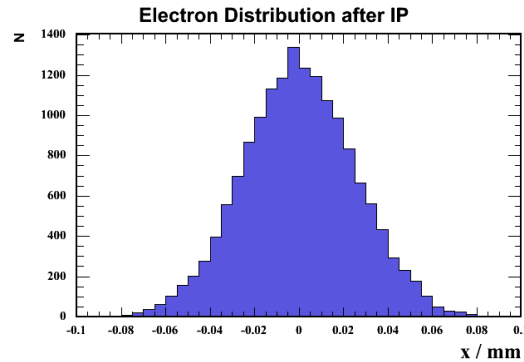


Figure 10: Spacial distribution of the scattered electrons just after the Compton IP

Left Helicity Configuration

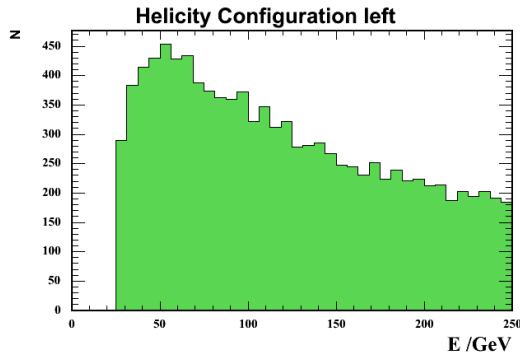


Figure 11: Energy distribution of the scattered electrons for the **left** handed helicity configuration.

Right Helicity Configuration

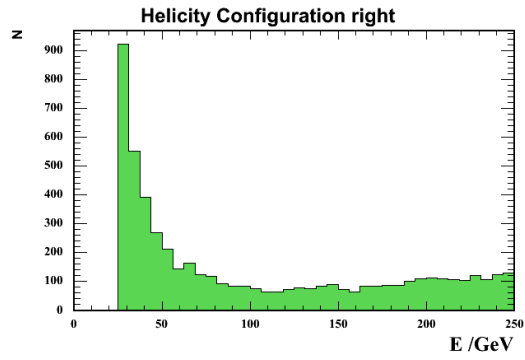


Figure 12: Energy distribution of the scattered electrons for the **right** handed helicity configuration.

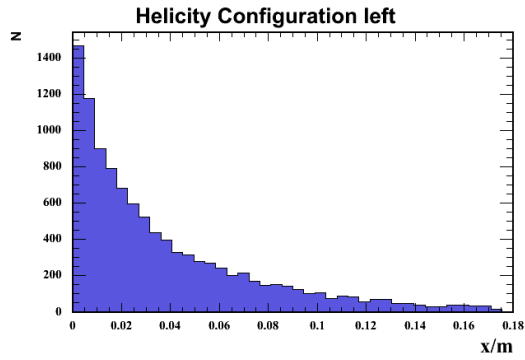


Figure 13: spacial distribution behind the spectrometer for the **left** handed helicity configuration.

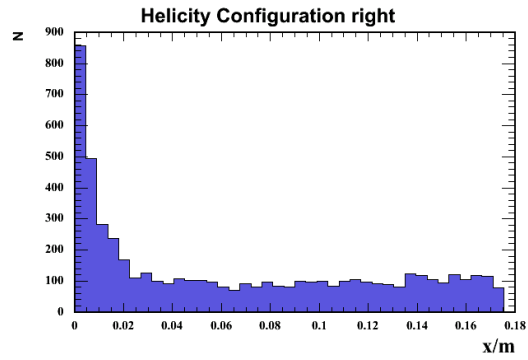


Figure 14: Spacial distribution behind the spectrometer for the **right** handed helicity configuration.

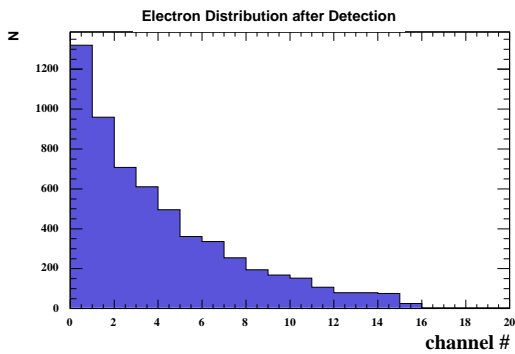


Figure 15: Spacial distribution into detector channels for the **left** handed helicity configuration.

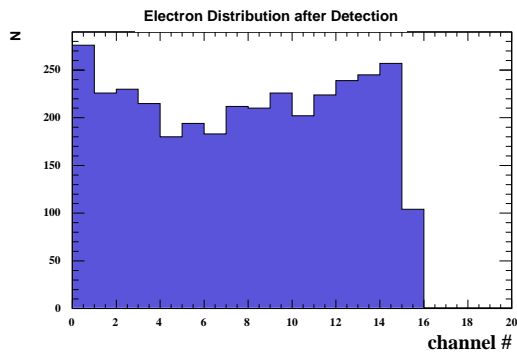


Figure 16: Spacial distribution into detector channels for the **left** handed helicity configuration.

In the detector channels each electron emits Cerenkov photons but only a small part of them are detected by the photo-cathode of the PM because of the quantum efficiency of the cathode material. All detected photons are counted up per each channel for the different configurations again. From this the asymmetry and finally the polarization can be determined for each channel. These processes can be seen in the following histograms.

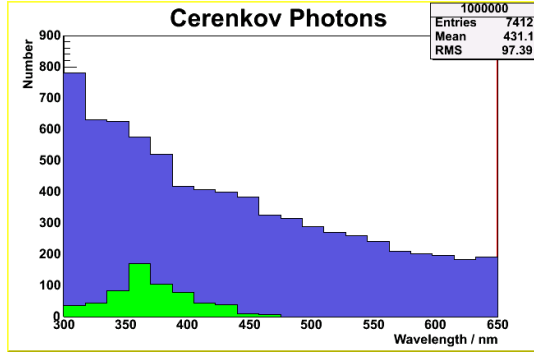


Figure 17: **Blue:** emitted Cerenkov photons; **Green:** detected photons

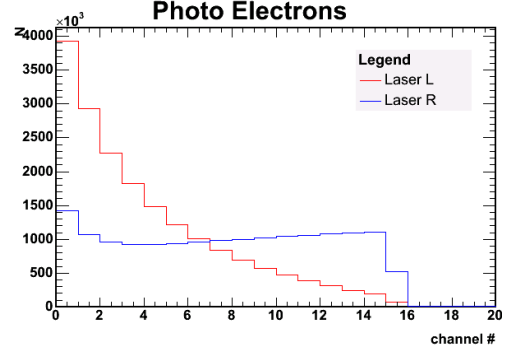


Figure 18: Distribution of the photo electrons for the two helicity configurations.

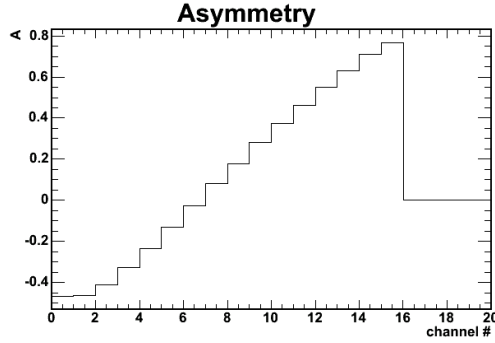


Figure 19: Asymmetry of the emitted photo electrons at the PM.

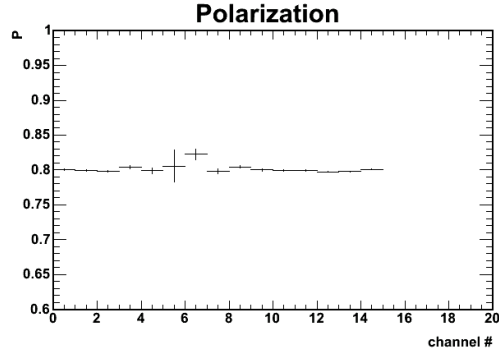


Figure 20: Polarization measured for each channel.

In building the weighted sum of all the measured single polarizations the polarization of the electron beam is determined:

$$P = 0.79957 \pm 0.00057$$

This result fits very well to the given polarization ($P = 0.8$).

A comparison of the asymmetries of the emitted photo electrons with the detected primary electrons shows that the ratio of the asymmetries is around the value one within the errors. In *Figure 21* one can see the ratio fitted with a straight line $f(x) = p_0 + p_1 \cdot x$ which shows that the ratio is indeed equal 1 within the errors.

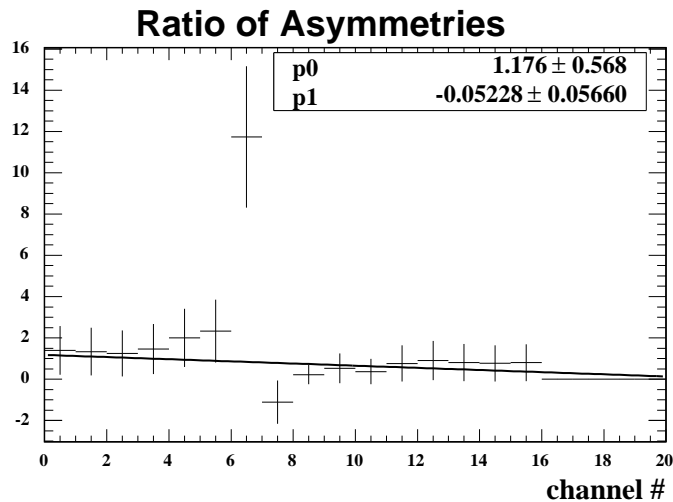


Figure 21: Cerenkov Radiation

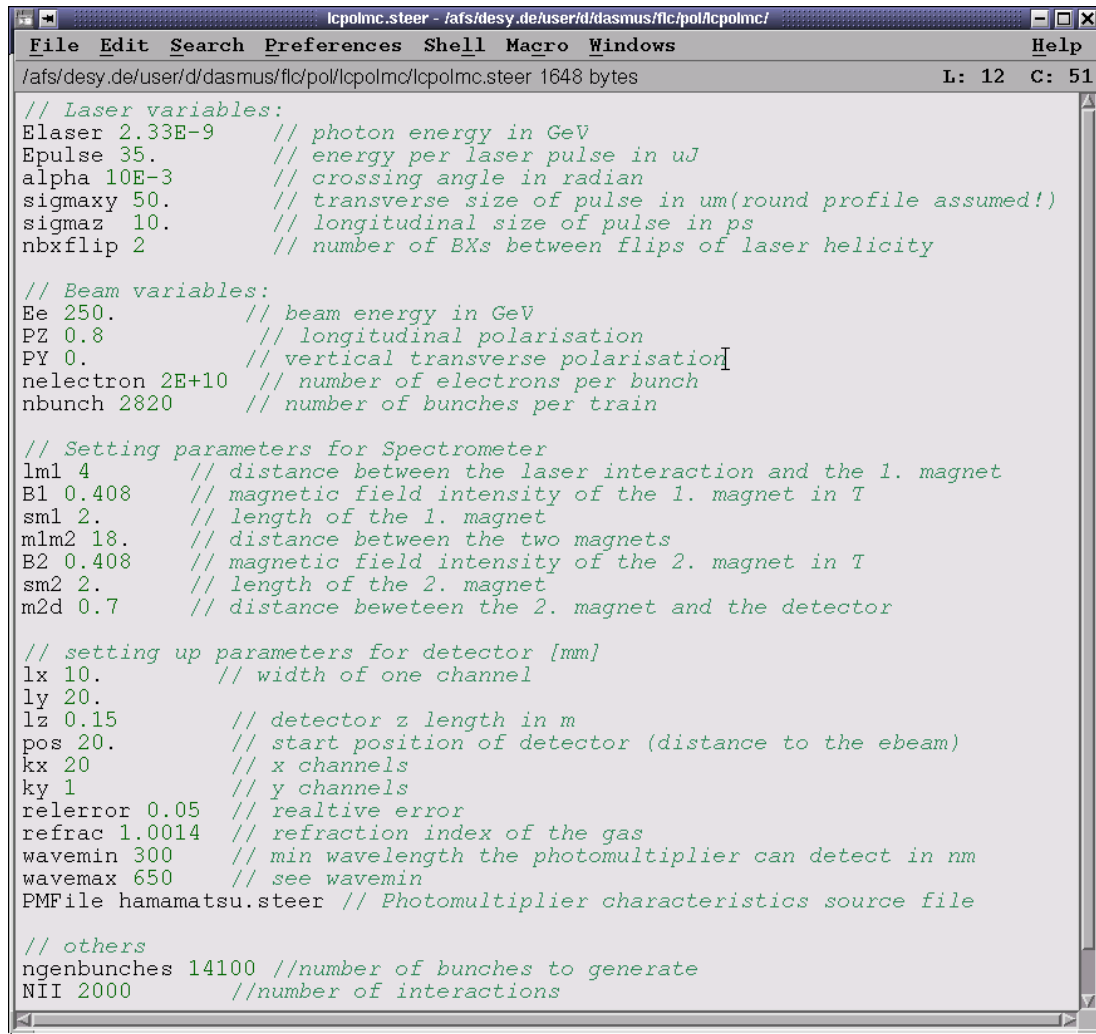
5.1 Systematical Errors

A detailed investigation of the systematic errors has still to be done. But in general one can expect a behavior similar to the SLD polarimeter at SLAC with an overall precision of $\frac{\Delta P}{P}$ 0.5% for the measurement of the beam polarization. The systematic effects from accelerator alignment, beam-beam interaction, bremsstrahlung and radiative corrections have been already discussed(see [1]). One of the most important issues will be the linearity of the outgoing signal which can be influenced by temperature, noise and radiation to mention only some aspects concerning the Cerenkov detector and photomultiplier tube. These systematic effects can be examined with this program now.

6 Summary

The up to date design for the Compton polarimeter to measure the longitudinal electron beam polarization with high precision is a 4-magnet chicane spectrometer with the detector design of the TESLA. The simulation of this polarimeter works satisfactory with the implemented Cerenkov gas detector and applied quantum efficiency of the PM. There are still details of the PM and the read-out electronics missing but in principle right now different designs for the detector or spectrometer can be studied.

7 Appendix: The Steering File

The image shows a screenshot of a text editor window titled 'lcpolmc.steer - /afs/desy.de/user/d/dasmus/flc/pol/lcpolmc/'. The window contains a steering file with various parameters and comments. The parameters are organized into sections: Laser variables, Beam variables, Spectrometer settings, detector settings, and others. Comments are provided for many parameters, explaining their units and physical meanings. The file is 1648 bytes long, and the cursor is at line 12, column 51.

```
lcpolmc.steer - /afs/desy.de/user/d/dasmus/flc/pol/lcpolmc/
File Edit Search Preferences Shell Macro Windows Help
/afs/desy.de/user/d/dasmus/flc/pol/lcpolmc/lcpolmc.steer 1648 bytes L: 12 C: 51

// Laser variables:
Elaser 2.33E-9 // photon energy in GeV
Epulse 35. // energy per laser pulse in uJ
alpha 10E-3 // crossing angle in radian
sigmaxy 50. // transverse size of pulse in um(round profile assumed!)
sigmaz 10. // longitudinal size of pulse in ps
nbxflip 2 // number of BXs between flips of laser helicity

// Beam variables:
Ee 250. // beam energy in GeV
PZ 0.8 // longitudinal polarisation
PY 0. // vertical transverse polarisation
nelectron 2E+10 // number of electrons per bunch
nbunch 2820 // number of bunches per train

// Setting parameters for Spectrometer
lm1 4 // distance between the laser interaction and the 1. magnet
B1 0.408 // magnetic field intensity of the 1. magnet in T
sm1 2. // length of the 1. magnet
mlm2 18. // distance between the two magnets
B2 0.408 // magnetic field intensity of the 2. magnet in T
sm2 2. // length of the 2. magnet
m2d 0.7 // distance beweteen the 2. magnet and the detector

// setting up parameters for detector [mm]
lx 10. // width of one channel
ly 20.
lz 0.15 // detector z length in m
pos 20. // start position of detector (distance to the ebeam)
kx 20 // x channels
ky 1 // y channels
relerror 0.05 // realtive error
refrac 1.0014 // refraction index of the gas
wavemin 300 // min wavelength the photomultiplier can detect in nm
wavemax 650 // see wavemin
PMFile hamamatsu.steer // Photomultiplier characteristics source file

// others
ngenbunches 14100 //number of bunches to generate
NII 2000 //number of interactions
```

Figure 22: Example of a steering file

In Figure 22 an example of a running steering file is shown. Actually it was used to produce the results in the sections above. The first word in a line is always the keyword and after a space has to stand the value the variable of the keyword shall become. The order of the keywords doesn't matter but only one per line. There are comments allowed after '// 'and will be ignored during the read out. The next table explain all the used keywords of the different parameters.

Explanation of the keywords

Photon Beam	
Elaser	laser beam energy in GeV
Epulse	energy per laser pulse in μJ
alpha	crossing angle of the laser beam and the electron beam in radian
sigmaxy	transverse size of the laser pulse in μM (round profile assumed)
sigmaz	longitudinal size of the laser pulse in ps
nbxflip	number of bunch crossings after which the laser helicity shall flip
Electron Beam	
Ee	electron beam energy in GeV
PZ	longitudinal beam polarization of the electron beam ($-1 \leq PZ \leq 1$)
PY	vertical transverse polarization of electron beam (at ILC PY = 0)
nelectron	number of electrons per bunch
nbunch	number of bunches per train
Spectrometer	
lml	distance between the Compton interaction point and the first dipole magnet behind
B1	magnetic field intensity of the first magnet after the IP in T
sm1	length of the first magnet after the IP in m
B2	magnetic field intensity of the second magnet after the IP just before the detector array in T
sm2	length of the second magnet
m2d	distance between the 2. magnet and the detector in m
Detector	
lx	width of a channel of the detector array in mm
ly	height of a channel of the detector array in mm
lz	length of a channel (gas tube) in m
pos	distance between the first detector channel and unscattered beam in mm
kx	number of channels in the x-direction
ky	number of channels in the y-direction
relerror	relative error used for Gaussian smearing of the detected values
refrac	refraction index of the gas in the Cerenkov gas tubes
wavemin	minimum wavelength the PM can detect in nm
wavemax	maximum wavelength the PM can detect in nm
PMFile	file name of the file containing the properties of the used PM (not finished yet)
Other	
ngenbunches	number of bunches which shall be generated and cross the IP
NII	number of maximum interactions per bunch crossing

8 References

- [1] Gharibyan, Meyners, Schueler: The TESLA Compton Polarimeter
- [2] Gharibyan, Meyners, Schueler: Upstream Polarimeter Update (ILC Workshop, Vienna 2005)
- [3] Leo: Techniques for Nuclear and Particle Physics Experiments
- [4] Flyckt, Marmonier: Photomultiplier tubes

